



# Recent progress of Pd/zeolite as passive NO<sub>x</sub> adsorber: Adsorption chemistry, structure–performance relationships, challenges and prospects

Ce Bian<sup>a</sup>, Dan Li<sup>a</sup>, Qian Liu<sup>a</sup>, Shoute Zhang<sup>a</sup>, Lei Pang<sup>b</sup>, Zhu Luo<sup>c</sup>, Yanbing Guo<sup>c</sup>, Zhen Chen<sup>a,\*</sup>, Tao Li<sup>a,\*</sup>

<sup>a</sup> Key Laboratory of Material Chemistry for Energy Conversion and Storage, Ministry of Education, Hubei Key Laboratory of Material Chemistry and Service Failure, School of Chemistry and Chemical Engineering, Huazhong University of Science and Technology, Wuhan 430074, China

<sup>b</sup> DongFeng Trucks R&D Center, Wuhan 430056, China

<sup>c</sup> Key Laboratory of Pesticide and Chemical Biology of Ministry of Education, Institute of Environmental and Applied Chemistry, College of Chemistry, Central China Normal University, Wuhan 430079, China

## ARTICLE INFO

### Article history:

Received 7 February 2021

Revised 21 April 2021

Accepted 30 July 2021

Available online 5 August 2021

### Keywords:

Emission control

Pd/zeolite

Passive NO<sub>x</sub> adsorber

NO<sub>x</sub> storage

Cold start

## ABSTRACT

Due to the technology limitation and inferior deNO<sub>x</sub> efficiency of urea selective catalytic reduction (SCR) catalysts at low temperatures, passive NO<sub>x</sub> adsorber (PNA) for decrease of NO<sub>x</sub>, CO and hydrocarbons (HCs) during “cold start” of vehicles was proposed to meet the further tighten NO<sub>x</sub> emission regulations in future. Among them, Pd modified zeolite PNA materials have received more attention because of their excellent NO<sub>x</sub> storage capacity, anti-poisoning and hydrothermal stability and since Pd/zeolite PNA was proposed, a variety of advanced characterization methods have been applied to investigate its adsorption behavior and structure–performance relationship. The comprehension of the active sites and adsorption chemistry of Pd/zeolite PNA was also significantly improved. However, there are few reviews that systematically summarize the recent progress and application challenges in atomic-level understanding of this material. In this review, we summarized the latest research progress of Pd/zeolite PNA, including active adsorption sites, adsorption mechanism, material physicochemical properties, preparation methods, storage and release performance and structure–performance relationships. In addition, the deactivation challenges faced by Pd/zeolite PNA in practical applications, such as chemical poisoning, high temperature hydrothermal aging deactivation, etc., were also discussed at the micro-level, and some possible effective countermeasures are given. Besides, some possible improvements and research hotspots were put forward, which could be helpful for designing and constructing more efficient PNA materials for meeting the ultra-low NO<sub>x</sub> emission regulation in the future.

© 2021 Published by Elsevier B.V. on behalf of Chinese Chemical Society and Institute of Materia Medica, Chinese Academy of Medical Sciences.

## 1. Introduction

Nitrogen oxides (NO<sub>x</sub>) is a notorious pollutant from vehicle emissions [1,2], which has been proven to cause various environmental and health problems [3–6]. Diesel vehicles contribute a large proportion of road NO<sub>x</sub> emissions due to their oxygen-rich lean combustion and high combustion temperature [7]. Therefore, increasingly stringent emission regulations for diesel vehicles have been proposed in major countries and regions around the world [2,8,9]. In recent years, selective catalytic reduction (SCR) with NH<sub>3</sub> as the reducing agent has been regarded as the most efficient tech-

nology to reduce NO<sub>x</sub> emissions in diesel vehicles [10–12]. Oxide materials (e.g., V<sub>2</sub>O<sub>5</sub>-WO<sub>3</sub>-TiO<sub>2</sub>) and metal modified zeolite (e.g., Cu/ZSM-5, Fe/SSZ-13 and Cu/SSZ-13) have been proven as highly efficient SCR catalyst [13–15]. Zeolite-based catalysts have received more attention because of their broader windows temperature and better hydrothermal stability [16,17], especially the Cu modified zeolite with small pore size reported in recent years, which exhibits a high NO<sub>x</sub> conversion rate in the range of 200 °C to 600 °C [18–20]. However, the state-of-the-art Cu/SSZ-13 catalyst still faces a “150 °C challenge” concerning its inferior low-temperature activity (< 150 °C) during the vehicle cold-start period. In addition, urea is difficult to decompose to NH<sub>3</sub> below 180 °C, which sets a technological limit to the applications of the Urea-SCR process at low temperatures [12,21,22]. Overall, the SCR system currently on

\* Corresponding authors.

E-mail addresses: zhende\_888@126.com (Z. Chen), taoli@hust.edu.cn (T. Li).

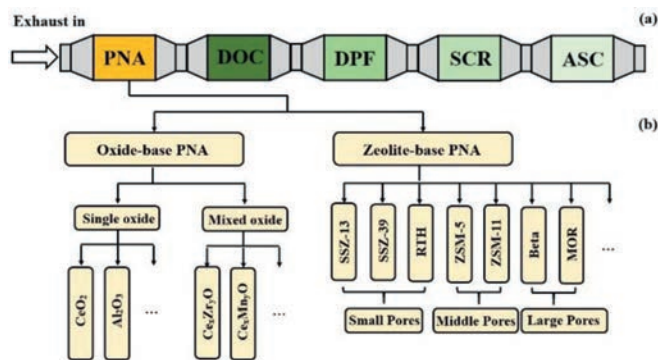


**Fig. 1.** (a) The relative installation position of PNA and SCR in diesel engine exhaust  $\text{NO}_x$  emission control system. (b) The main classification of PNA catalyst.

diesel vehicles exhibits poor working efficiency or even complete failure at low temperature, which may cause a large amount of  $\text{NO}_x$  emission during diesel vehicle “cold start” (*i.e.*, engine starting before the SCR catalyst is operation) [23,24].

To deal with the dilemma faced by SCR system, a new device namely passive  $\text{NO}_x$  adsorber (PNA) has been proposed [25–27]. The PNA material adsorbs  $\text{NO}_x$  at low a temperature and releases it until the SCR system is awakened. Currently, two types of materials were considered as PNA candidates (Fig. 1). Transition metal oxide and zeolite are often used as supports and the transition metals (usually precious metal, Pt, Pd and Ag) are used as active adsorption sites [22]. Although the zeolite-based PNA was proposed later than oxide based PNA, it still subjects to wider attention. This is own to its better  $\text{NO}_x$  storage capacity, poisoning resistance and hydrothermal stability [22,28]. At present, most zeolite-based PNA used Pd as the active species, which is attributed to the moderate binding strength of Pd species and  $\text{NO}_x$ . Therefore, Pd/zeolites can release previously stored  $\text{NO}_x$  in a suitable temperature window. In another word, Pd/zeolite material has become one of the most potential PNA candidate materials.

Although Pd/zeolite PNA materials have many advantages, there are still some problems to be solved before it is practical: i) The adsorption chemistry and structure-performance relationships of Pd/zeolite PNA need to be further studied and improved; ii) Expensive prices due to the use of precious metal; iii) Challenges posed by harsh work condition (*e.g.*, chemical poisoning and hydrothermal aging). Thus, a variety of strategies to promote the development of Pd/zeolite PNA have been adopted by researchers, and multiple advanced characterization methods were used to investigate the structure-activity relationship and the  $\text{NO}_x$  adsorption and desorption mechanism. Based on the development of theory, some strategies have been applied to increase the storage capacity and utilization efficiency of precious metal, the non-precious metal PNA materials were also proposed to reduce catalyst costs [29]. In addition, the deactivation caused by long-term working was also studied and some countermeasures have been proposed. At present, some researchers have summarized the research results of low-temperature  $\text{NO}_x$  adsorption materials from types, performance, adsorption sites and effect by working condition, respectively [22,30,31]. However, we believe that the latest understanding of the adsorption mechanism, preparation and practice of Pd/zeolite with high adsorption capacity still need to be supplemented.

In this review, we discussed the research hotspots and progress of Pd/zeolite PNA materials from the following aspects: adsorption chemistry, structure-performance relationships and challenges and prospects. The distribution of active species,  $\text{NO}_x$  adsorption chemistry, the influence of the synthesis process and the deactivation

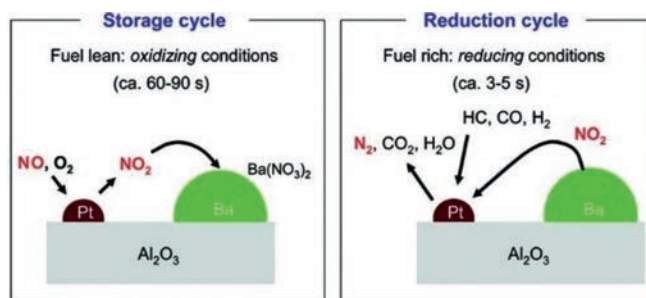


**Fig. 2.** A brief pictorial representation of the mechanism of NSR. Reprinted with permission [34]. Copyright 2009, American Chemical Society.

chemistry are discussed at the micro-level. These points may provide some references to the design of high-performance PNA materials and further mechanism research on Pd/zeolite materials in the future. Finally, some research prospects were proposed.

## 2. Development of de $\text{NO}_x$ technology

Due to the operating characteristics of lean burn and high temperature, the de $\text{NO}_x$  technology for diesel vehicle exhaust has received widespread attention long ago. With the continuous updating of emission regulations in countries around the world, the de $\text{NO}_x$  technology is also developing rapidly. In this section, we will review the  $\text{NO}_x$  emission control technology used in diesel vehicle exhaust, which can help understand the importance of PNA.

### 2.1. Direct decomposition of NO

Nitric oxide can be directly decomposed into nitrogen and oxygen in the presence of a catalyst. The process can be represented by the following chemical equation (Eq. 1).



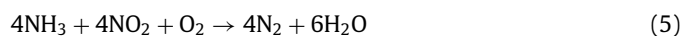
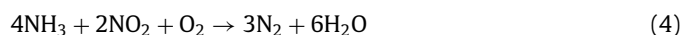
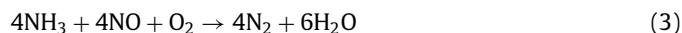
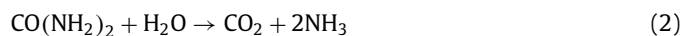
Iwamoto *et al.* [32] found that Cu/ZSM-5 can efficiently catalyze this reaction. In addition, Noble metals modified oxide was also found to be suitable for this reaction. The direct decomposition reaction of NO does not require an additional reducing agent, which makes the technical route simpler and environmentally friendly. However, the progress of the reaction may be inhibited by high oxygen concentration, which is not conducive to working in a lean diesel exhaust atmosphere. In another hand, the hydrothermal stability and  $\text{SO}_2$  tolerance of the catalyst is another issue that needs to be paid attention to. Therefore, this technology still needs further research.

### 2.2. $\text{NO}_x$ storage reduction

$\text{NO}_x$  storage reduction (NSR) is another mature de $\text{NO}_x$  technology for automobile exhaust. The NSR catalysts usually consist of supports, precious metals (*e.g.*, Pt, Pd and Rh) and  $\text{NO}_x$  storage species (*e.g.*, alkali metal oxides and barium species) [33,34]. Generally, NSR catalyst needs to work under the condition of the lean-rich combustion cycle.  $\text{NO}_x$  is adsorbed and stored in the lean burn stages, and reduced in the rich burn stages. The working mechanism of NSR catalyst based on  $\text{Al}_2\text{O}_3$ -Pt-Ba and an illustrative sketch of lean-rich cycles are given (as shown in Fig. 2) [34]. At present, there are still some problems in NSR technology that need to be resolved: i) The  $\text{SO}_2$  tolerance of the catalyst needs to be improved urgently; ii) The thermal poisoning of the catalyst needs to be suppressed; iii) The rich-lean cycle working condition required by the NSR catalyst poses a challenge to engine control technology.

### 2.3. Selective catalytic reduction

SCR is an effective NO<sub>x</sub> removal technology under oxygen-rich conditions, NO<sub>x</sub> is selectively reduced to non-toxic N<sub>2</sub> in the presence of a catalyst. According to different reducing agents, SCR technology can also be subdivided into H<sub>2</sub>-SCR, HC-SCR, NH<sub>3</sub>-SCR and solid selective catalytic reduction (SSCR) [35–38]. At present, NH<sub>3</sub>-SCR technology is considered to be the most efficient and economical exhaust NO<sub>x</sub> removal technology [39]. Urea is usually used as a precursor, and it decomposes at high temperatures to produce ammonia. The main chemical reactions involved in Urea-SCR technology are as follows Eqs. 2–5.



At present, transition metal oxides and transition metal modified zeolites have been used as the catalyst for the NH<sub>3</sub>-SCR reaction [10]. The transition metal modified zeolite catalyst has a wide temperature window, high catalytic activity, and excellent hydrothermal stability. However, Urea-SCR technology still faces some problems, such as NO<sub>x</sub> emission during “cold start” [12,21,22]. At such a low temperature, not only the activity of the catalyst is poor, but urea is also difficult to decompose into NH<sub>3</sub>. To provide a reducing agent for the reaction at low temperatures, SCR technology based on solid NH<sub>3</sub> precursors is proposed, namely solid selective catalytic reduction (SSCR) [40]. However, SSCR technology requires additional heating and quantitative injection device, which undoubtedly increases the complexity of the exhaust gas treatment system.

### 2.4. Passive NO<sub>x</sub> adsorber

PNA is another technology proposed to solve the low temperature dilemma of SCR. Generally, PNA materials adsorb NO<sub>x</sub> at low temperatures, and release it at high temperatures [22,30]. After this process is over, the PNA material will return to a state where it can adsorb NO<sub>x</sub> again. Different from NSR, the PNA+SCR strategy does not need to work under the conditions of lean-rich combustion cycle, which means that the PNA+SCR route has great application potential in lean-burn engines. Currently, there are two types of materials proposed as candidates for PNA, namely oxide-based materials and zeolite-based materials. Although zeolite-based PNA was proposed later than oxide-based PNAs, their excellent NO<sub>x</sub> storage capacity, anti-poisoning and hydrothermal aging properties have quickly attracted widespread attention. Chen *et al.* [28] compared the NO<sub>x</sub> storage capacity and SO<sub>2</sub> tolerance of several Pd/zeolite and Pd/CeO<sub>2</sub> materials, proving the advantages of Pd/zeolite. Nowadays, Pd/zeolite has become a current research hotspot in the field of PNA, especially, especially about the adsorption chemistry, structure-performance relationships of materials [22,30].

## 3. Active adsorption sites in Pd/zeolite PNA

According to previous studies [41–44], Pd is considered as the most suitable PNA active species. Understanding the adsorption mechanism of NO<sub>x</sub> on Pd promoted zeolite can greatly help the designing and adjusting of PNA which has high NO<sub>x</sub> storage performance. However, the adsorption of NO<sub>x</sub> on Pd/zeolite is a series of



Fig. 3. The interaction of different Pd species with NO. Reprinted with permission [45]. Copyright 2017, American Chemical Society.

complex chemical processes [45], this is due to the diversity of Pd species on the zeolite framework. Therefore, the researchers discussed the distribution and role of adsorption sites on Pd/zeolite in detail. In this section, we will summarize the Pd species on the zeolite framework and their interaction with NO<sub>x</sub>.

Pd species have been proved to exist on the zeolite framework in multiple valence states and their distribution may be affected by the chemical environment of zeolite [46]. Generally, most Pd species distributes as Pd<sup>2+</sup> cations and PdO<sub>x</sub> clusters [45,47,48]. Pd<sup>0</sup> clusters have also been supported to exist on the surface of zeolite framework, which may be produced by the reduction of Pd<sup>2+</sup> cations [46,49]. Besides, “naked” Pd<sup>+</sup> was identified by diffuse reflection infrared Fourier transform spectroscopy (DRIFTS) on multiple zeolite frameworks [45]. Additionally, the tetravalent Pd species has been also confirmed by X-ray diffraction (XRD) to exist in Pd modified zeolite [48].

Despite the complexity of the Pd species, well-dispersed Pd cations are considered as most efficiently active species for zeolite-based PNA [50]. Therefore, investigating the interaction between Pd cation sites and NO<sub>x</sub> has become the key to understanding the mechanism of NO<sub>x</sub> uptake and release. Chen *et al.* [28] studied the NO<sub>x</sub> adsorption behavior on different Pd promoted zeolite. In addition to the NO<sub>x</sub> adsorbed on the zeolite framework, linear nitrosyl species formed by the adsorption of NO by dispersed Pd<sup>2+</sup> were also supported by DRIFTS, which was consistent with previous reports [48,51–53]. Zheng *et al.* [45] discussed the existence and role of Pd species in more deeply. The Fourier transform infrared spectrometer (FTIR) using CO as a molecular probe revealed the existence of multiple Pd species. In addition to the isolated Pd(II) sites (Z-Pd<sup>2+</sup>Z<sup>-</sup> and Z-H<sup>+</sup>[Pd(OH)]<sup>+</sup>Z<sup>-</sup>, Z<sup>-</sup> stands for the ion-exchange site), Pd<sup>+</sup> sites and PdO<sub>x</sub> and PdO particles on external surfaces, charge compensating isolated and oligomeric Pd-oxo ions have also been confirmed to exist in a variety of Pd/zeolite. Isolated Pd(II) sites and Pd<sup>+</sup> sites are considered responsible for NO adsorption, Z-Pd<sup>2+</sup>Z<sup>-</sup> and Pd<sup>+</sup> sites can store NO directly by forming a complex, while Z-H<sup>+</sup>[Pd(OH)]<sup>+</sup>Z<sup>-</sup> is considered to be reduced to Pd<sup>+</sup> sites and produce NO<sub>2</sub>, as shown in Fig. 3. In addition, the Pd(IV)O<sub>2</sub> species is also believed to be responsible for the formation of NO<sub>2</sub>.

The interaction between Pd species and NO<sub>x</sub> on the zeolite framework is not simple adsorption behavior, on the contrary, a series of complex chemical processes occur together, which will also affect the state of the Pd species. Zheng *et al.* [45] proposed the reduction of divalent Pd in Z-H<sup>+</sup>[Pd(OH)]<sup>+</sup>Z<sup>-</sup> and tetravalent Pd in PdO<sub>x</sub> cluster by NO, at the same time, the valence of Pd species decreases. The same viewpoint was also proposed by Porta *et al.* [54]. Besides, they pointed out that the oxidation-reduction reaction has an impact on NO<sub>x</sub> storage performance, the generation of NO<sub>2</sub> was considered to improve the PNA performance by forming a stable nitrate. Mei *et al.* [55] studied monomeric and dimeric

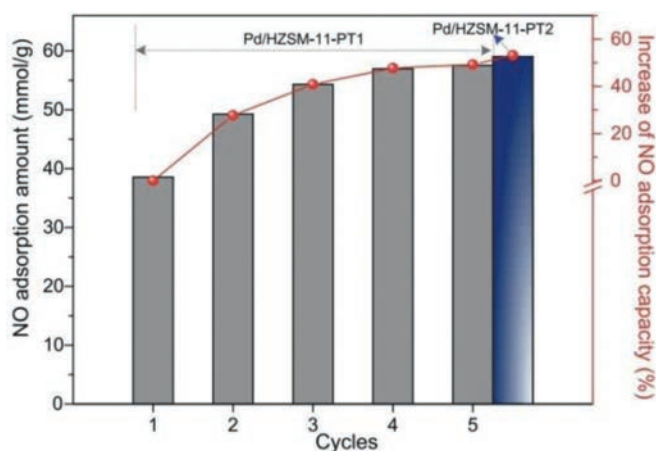


Fig. 4. NO adsorption capacity on Pd/HZSM-11 after different adsorption and release cycles. Reprinted with permission [56]. Copyright 2020, Elsevier.

Pd sites on HBEA. They suggested that the oxidation of CO at the dimeric  $[\text{Pd}^{\text{II}}\text{-O-Pd}^{\text{II}}]^{2+}$  sites was considered feasible. Similarly, NO can be oxidized at the sites of monomer  $\text{Pd}^{\text{II}}\text{O}$  and dimeric  $[\text{Pd}^{\text{II}}\text{-O-Pd}^{\text{II}}]^{2+}$ , and resulting in Pd species change.

In short, Pd species transformation is proven during the PNA process, and that always leads to changes in  $\text{NO}_x$  storage performance, undoubtedly. Yu *et al.* [56] proposed the increase in  $\text{NO}_x$  storage capacity by pretreatments under simulated exhaust atmosphere (as shown in Fig. 4), which was attributed to the oxidation of the Pd(II) species in the  $\text{NO}_x$  atmosphere. However, deactivation caused by  $\text{NO}_x$  atmosphere was also reported [57]. Currently, the effect of  $\text{NO}_x$  on Pd species has not been fully understood and it may be also affected by many factors such as temperature and concentration. Therefore, in-depth research based on advanced characterization is urgently needed. In addition, it is worth mentioning that non-noble metal active species (such as SSZ-13 modified by cobalt [29]) used to replace expensive Pd have been proposed and used to modify SSZ-13. However, the zeolite PNA modified by non-precious still need to be further optimized in terms of performance and durability, and the functions and properties of these active species also need to be further investigated.

## 4. Influence factors of Pd/zeolite PNA performance

### 4.1. Effect of synthesis methods on the $\text{NO}_x$ storage performance of Pd/zeolite PNA

Currently, various methods were reported to load a transition metal on zeolite supports, such as ion exchange, impregnation and one-pot method [20,58–60]. Each of the methods has its characteristics and affects the appearance and performance of the catalyst significantly. In this part, we summarized several common metal-zeolite preparation methods and their application in the preparation of Pd/zeolite PNA. Additionally, their differences, advantages and disadvantages are also discussed.

#### 4.1.1. Pd/zeolite PNA prepared by ion-exchange methods

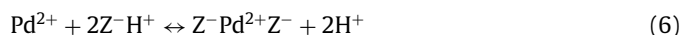
The ion-exchange method generally mixes the prepared precursor with the supported zeolite carrier, and after proper mixing treatment, the metal ions are finally exchanged to the cationic sites on the zeolite framework. Generally, solution precursors are more commonly used, which is also called the aqueous ion-exchange method (AIE). At present, many articles have reported the use of AIE to prepare the Pd/zeolite PNA materials [45,50,54,57,61–64]. The AIE method can simply realize metal modification, and it has been proved to be able to prepare high-efficiency Pd/zeolite PNA

with large and medium pore sizes. On another hand, the solid-state precursors can also be used to ion-exchange process of zeolite, namely solid-state ion-exchange (SSIE). This technology was reported by Rabo *et al.* firstly [65]. SSIE avoids the use of solution precursors and helps reduce synthetic wastewater. Currently, there have been reports on the use of SSIE to synthesize Pd/SSZ-13 PNA materials, but this material exhibits poor adsorption performance [50]. The author proposed a possible reason for the failure of solid-state ion exchange: In SSIE process,  $\text{PdCl}_2$  precursor migrate to the zeolite framework by forming a gas phase multimeric, however, since the gaseous molecule is presumably  $\text{Pd}_6\text{Cl}_{12}$  which size is approximately 7.6 Å (bigger than the pore size of SSZ-13), the introduction of the Pd precursor in SSZ-13 is prevented.

#### 4.1.2. Pd/zeolite PNA prepared by impregnation methods

Impregnation is another common method to load a metal to zeolite support. Similar to the AIE method, the impregnation method also adopts a strategy of mixing carrier and liquid precursor. The difference is that the impregnation method usually removes the water in the precursor solution by drying instead of filtering. At present, two methods wet impregnation (WI) and incipient wetness impregnation (IWI) have been reported to synthesize Pd/zeolite PNA materials [47,50,56,66–75]. In previous reports, conventional ion exchange and impregnation methods often failed to disperse Pd species on small pore zeolites. Some researchers suggest that this is due to the hydrated ion Pd difficult to enter the zeolite pores (such as SSZ-13,  $\approx 3.8$  Å) [50].

To respond this problem, Khivantsev *et al.* [76] proposed a new strategy to achieve atomic dispersion of Pd species in the SSZ-13 framework, namely “modified ion exchange”. The “modified ion-exchange” was improved from the IWI method, but there are significant differences. They used the  $\text{NH}_4\text{-SSZ-13}$  or  $\text{H-SSZ-13}$  as zeolite support, and the thick paste of Pd precursor and zeolite powder is stirred and calcined at 650 °C. The Pd nitrates dissolved in ammonia is used as a precursor, which is considered to be the key strategies of completely ion-exchange. The authors also proposed an explanation of the mechanism by which this strategy promotes ion exchange. First, they proposed another mechanism that hinders the progress of ion exchange. For H-form zeolites, the ion exchange in the pores has the following reversible processes (Eq. 6):



However, the highly acidic environment of the zeolite micropores provides resistance to the ion exchange process. The strategy of using  $\text{NH}_3$ -form zeolite and nitrate Pd precursor can easily remove the generated cations (the decomposing temperature of  $\text{NH}_4\text{NO}_3$  is only 180 °C) and lead to complete ion exchange. The X-ray absorption near-edge structure (XANES) region of the extended X-ray absorption fine structure (EXAFS) spectrum (Fig. 5) indicates that the Pd cations are present in the divalent state. The full EXAFS spectrum showed that the Pd-O-Pd bond cannot be detected. The effectiveness of this method is attributed to the volatility of the product ( $\text{NH}_4\text{NO}_3$ ) during the ion exchange, which led to the constant promotion of reaction equilibrium. In addition, the authors proposed the zeolite support with a low Si/Al ratio (SAR) also assist in the dispersion of Pd.

All in all, several synthesis methods of Pd/zeolite PNA have been reported. Ion-exchange method and impregnation generally implement the modification of the zeolite support by mixing, stirring, calcination and other methods. The simple solution ion exchange method is easy to industrialize due to its simple steps and is an effective candidate for the synthesis of large and mesoporous Pd/zeolite PNA materials. Currently, high-performance Pd/zeolite with small pores size synthesized by a modified impregnation method has also been reported. Considering the production of a large amount of wastewater in the two-step method (that is, the

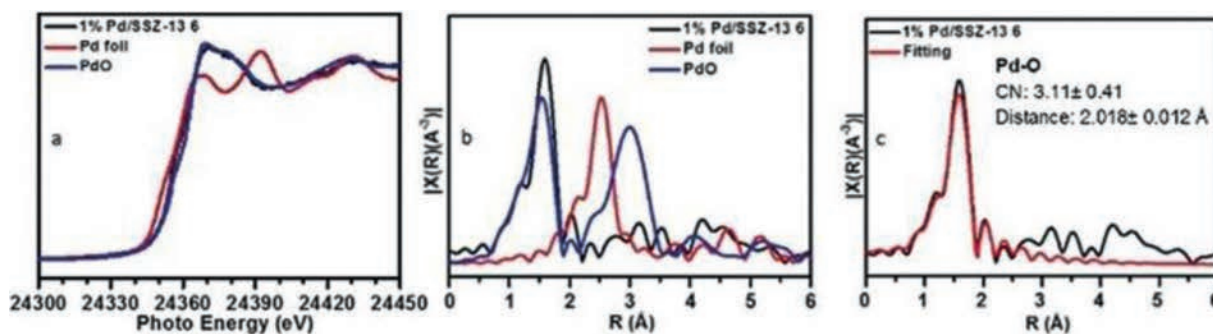


**Fig. 5.** (a) XANES region of the 1 wt% Pd/SSZ-13, (b) Fourier transform of  $k^2$ -weighted EXAFS spectra in the R-space for 1 wt% Pd/SSZ-13, reference Pd foil and PdO, (c) Coordination number and bond lengths of Pd-O in 1 wt% Pd/SSZ-13. Reprinted with permission [76]. Copyright 2018, Wiley-VCH Verlag GmbH & Co. KGaA.

**Table 1**

Zeolite-based PNA: types, synthesis methods, advantages and disadvantages.

Zeolite	Precursors	Synthesis methods	Advantages and disadvantages	Storage stability ( $\mu\text{mol/g}_{\text{cat}}$ )	Ref.
SSZ-13	$\text{Pd}(\text{NO}_3)_2$	IWI	Excellent anti-poisoning performance and HTA tolerance	8.9-250	[28,49,50,75,76,87,103]
		WI		25.8	[50]
		AIE		25.4-147	[50,57,61,62]
	$\text{PdCl}_2$	SSIE	17.1	[50]	
	AIE	91.4	[45,62]		
SSZ-39	$\text{Co}(\text{CH}_2\text{COOH})_2$	AIE	Low cost	27.3	[29]
	$\text{Pd}(\text{NO}_3)_2$	IWI	Superior stability, but expensive and irreplaceable SDA	84.8	[66]
RTH	$\text{Pd}(\text{NO}_3)_2$	IWI	Prone to Pd species aggregation	30.4	[66]
ZSM-5	$\text{Pd}(\text{NO}_3)_2$	IWI	The preparation is simple, and the active species are easier to disperse.	28-195	[47,67]
		AIE		24.5-93	[54,57,61,63]
		AIE		102.5	[45]
ZSM-11	$\text{Pd}(\text{NO}_3)_2$	IWI		59.03	[56]
MCM-22	$\text{Pd}(\text{NO}_3)_2$	AIE		62	[64]
DS-ITQ-2	$\text{Pd}(\text{NO}_3)_2$	AIE		64	[64]
BEA	$\text{Pd}(\text{NO}_3)_2$	IWI	The preparation is simple, and the active species are easier to disperse.	20-287	[68-74]
		WI		N/A	[75]
		AIE		38	[54]
		AIE		110.8	[45]
FER	$\text{Pd}(\text{NO}_3)_2$	AIE		24	[54]
MOR	$\text{Pd}(\text{NO}_3)_2$	AIE		20	[54]

zeolite support is synthesized first, and then the precursor is modified), a greener one-step method may be developed in the future.

#### 4.2. Effect of zeolite supports to $\text{NO}_x$ storage performance and stability

Currently, at least ten zeolite supports have been reported for the synthesis of Pd/zeolite PNA materials. These Pd/zeolite materials show different adsorption performance, because the zeolite supports determine the microscopic pore structure of the material and the chemical environment of the active site. We summarized the synthesis method and  $\text{NO}_x$  adsorption capacity of these materials, as shown in Table 1. In general, the zeolite supports can be divided into three types according to pore size (large, medium and small pores). Beta with large pores, ZSM-5 with mesopores and SSZ-13 with small pores are the current research hotspots. In this part, we will introduce the preparation and performance characteristics of these three kinds of Pd/zeolite, which will help to better understand the structure-activity relationship of Pd/zeolite.

Beta zeolite was synthesized by Wadlinger in 1967 firstly [77], which has three-dimensional micropores composed of 12-membered rings [78,79]. The Beta zeolite is widely used in petrochemical industry which is based on its good resistance to hydrothermal aging, acid resistance and coking tolerance. The synthesis of Pd/BEA PNA materials by impregnating and ion-exchange methods have been reported. The dispersion of Pd species on the BEA framework is easy, due to its large pore size. For the same reason, Pd/BEA also exhibits good hydrocarbons (HCs) tolerance.

Similar to BEA, Pd species can also simply be dispersed on ZSM-5, which can also be attributed to its larger pore size. The medium-sized pores composed of 10-membered rings [80] allow Pd/ZSM-5 to be synthesized through a simple ion exchange strategy.

Although Pd/zeolite with mesopores and macropores can be synthesized more simply, PNA materials with SSZ-13 as a carrier are still receiving extensive attention due to their excellent long-range performance, especially hydrothermal stability. However, as mentioned before, hydrated Pd ions is difficult to enter the narrow 8-membered ring of SSZ-13 [28]. Therefore, the synthesis of high-performance Pd/SSZ-13 PNA materials must adopt specific methods and precursors [76].

In addition to the type of zeolite support, the chemical environment of the framework also significantly affects the adsorption performance of the PNA material. It was reported that the SAR may significantly influence storage capacity and stability [81-83]. Mi-hai *et al.* [75] studied the  $\text{NO}_x$  storage performance of Pd/BEA and Pd/SSZ-13 with different SAR. The Pd/BEA samples with low SAR showed an obvious advantage in storage capacity. Moreover, the scanning transmission electron microscopy (STEM) indicates that Pd species tend to exist in the form of aggregation on the high SAR framework (as shown in Fig. 6.1), which means low Pd utilization. A similar trend is also observed in Pd/SSZ-13. Essentially, for a silica-alumina zeolite, a lower SAR contributes to providing more ion-exchange sites [76,82,84], which undoubtedly helps the existence and stability of isolated  $\text{Pd}^{2+}$  cations. In another hand, a lower SAR brings more abundant Brønsted acid sites, which can conducive to the stability of  $\text{Pd}^{2+}$  cations [83,85]. However, low

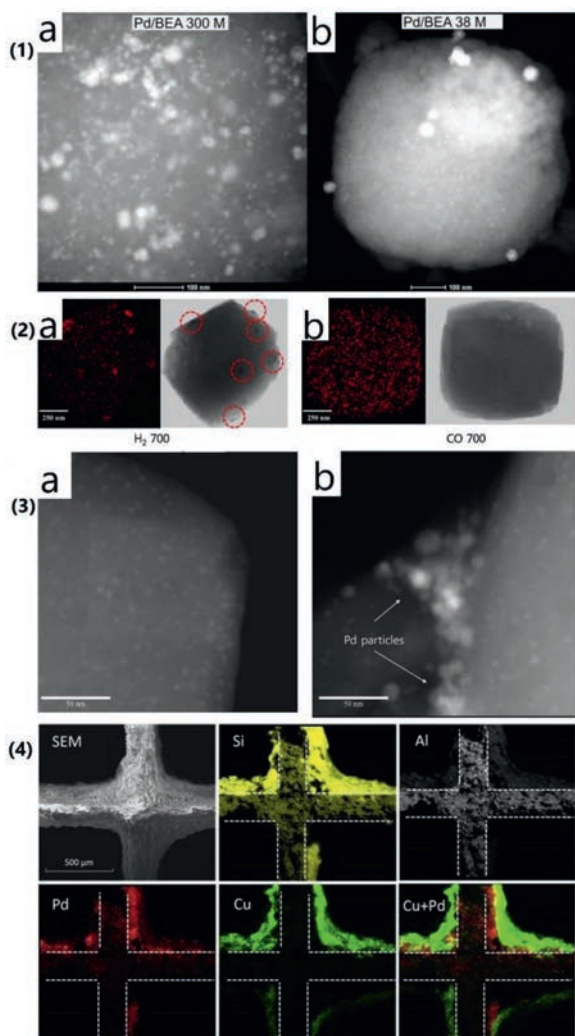


**Fig. 6.** (1) (a) STEM images of the Pd/BEA (SAR = 300) at 100 nm; (b) Pd/BEA (SAR = 38) at 100 nm. Reprinted with permission [75]. Copyright 2018, Springer Nature. (2) (Left) EDS mapping analysis for Pd and (Right) Z-contrast STEM image of (a) fresh and (b) HTA Pd/SSZ-13. Reprinted with permission [50]. Copyright 2017, Elsevier. (3) HAADF-STEM images of 700 °C treatment by (a) H<sub>2</sub> and (b) CO. Reprinted with permission [49]. Copyright 2019, Elsevier. (4) the SEM image of layered Pd/SSZ-13+Cu/SSZ-13 washcoat and EDS elemental mapping for Si, Al, Pd, Cu, and Cu + Pd. Reprinted with permission [107]. Copyright 2021, Elsevier.

SAR may cause the reduction of hydrothermal stability due to easier dealumination of the framework [86]. Therefore, it is necessary to adjust the SAR to an appropriate range to take into account both performance and stability.

#### 4.3. Effect of other components in exhaust gas on the NO<sub>x</sub> storage performance of Pd/zeolite

Pd species on the zeolite framework and their interactions with NO<sub>x</sub> have been discussed in Section 3. However, the adsorption behavior and mechanism of the actual Pd/zeolite PNA material are very complex because of the complex exhaust gas composition. Therefore, the adsorption behavior chemistry of PNA materials under complex conditions are very necessary. Here, we summarize the influence of several common exhaust gas components on PNA, as shown in Table 2.

##### 4.3.1. Effect of H<sub>2</sub>O on the PNA performance of Pd/zeolite

The impacts of water on PNA materials must be considered because of the humid environment of exhaust gas. Szanyi's group

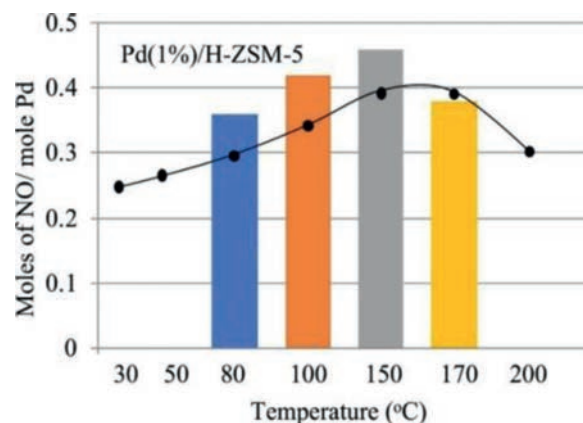


**Fig. 7.** Comparison of moles of NO / mole Pd at different uptake temperatures under the feed contained 7% H<sub>2</sub>O. Reprinted with permission [47]. Copyright 2018, Elsevier.

[45] studied the effect of H<sub>2</sub>O on different Pd modified zeolite. Their research results suggest that the dispersed Pd cations are less affected than other Pd species in a humid test condition. H<sub>2</sub>O severely inhibits the interaction between PdO<sub>x</sub> and NO<sub>x</sub>, but the adsorption performance of isolated Pd<sup>2+</sup> cations is almost unchanged. However, a deeper understanding of the adsorption behavior involving water was proposed by their subsequent studies [87], a Pd/SSZ-13 material rich in Pd ions was synthesized and used as a model material. The temperature program experiment result indicates that the NO<sub>x</sub> storage capacity of Pd<sup>2+</sup> cations decreases in the presence of H<sub>2</sub>O. But when water and CO exist at the same time, the storage capacity is almost unaffected. In fact, it does not contradict to the results of their previous studies, because CO was always added as a fixed component to simulate the real working conditions. In short, their results supported the advantages of Pd<sup>2+</sup> cation sites under humid working conditions.

To further study the role of H<sub>2</sub>O in the NO<sub>x</sub> adsorption process, Ambast *et al.* discussed the NO<sub>x</sub> adsorption behavior toward kinetic methods [47]. The NO<sub>x</sub> adsorption capacity of Pd/ZSM-5 was observed to correlate with temperature in the presence of water (as shown in Fig. 7). They attributed this trend to the decrease in H<sub>2</sub>O coverage with increasing temperature. Based on experimental results, two microkinetic schemes were developed to simulate the NO<sub>x</sub> adsorption behavior.

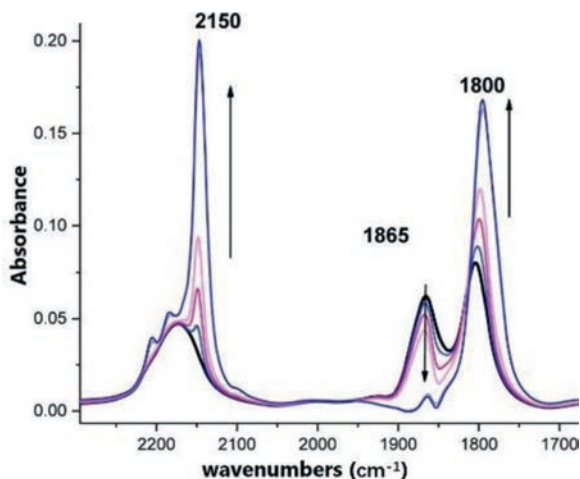
##### 4.3.2. Effect of CO on the PNA performance of Pd/zeolite

The CO in automobile exhaust is mainly produced from the incomplete combustion of fuel. As well known, CO may cause precious metal catalyst poisoning, especially at low temperatures [88,89], this may be because CO is easier to cause adsorption on precious metal species. Therefore, CO is also used to investigate the types of Pd species in zeolite [45]. Similarly, for Pd/zeolite PNA materials, the effect caused by CO must be carefully investigated.

In the zeolite-based PNA that has just been put forward soon, Vu *et al.* [68] studied the effect of CO on Pd/BEA during NO<sub>x</sub> adsorption. The temperature programmed experience showed that the introduction of CO led to a significant improvement of the NO<sub>x</sub> storage capacity and desorption temperature. The author attributes the change in adsorption behavior to the reduction of Pd<sup>2+</sup> cations by CO, because Pd sites with lower valence may bind NO<sub>x</sub> more tightly. This difference in adsorption strength can be attributed to the π back-donation effect strengthening the covalent bond strength. The experimental results of Gupta *et al.* [90] also support this view. The DRIFTS suggests the reduction of Pd<sup>2+</sup> sites to Pd<sup>+</sup> in the presence of CO. The stronger binding strength to NO of Pd<sup>+</sup> may be also supported by DFT calculations.

**Table 2**  
Other components in exhaust gas and their effect on PNA.

Components in the feed	Influence to active adsorption sites	Influence to storage and release performance	Ref.
O <sub>2</sub>	Promote the formation of nitrosyl species	Increase NO <sub>x</sub> adsorption capacity	[87]
H <sub>2</sub> O	Competitive adsorption with NO <sub>x</sub> Reduction of active sites in the presence of NO Damage to the zeolite framework at high temperature	May reduce NO <sub>x</sub> storage capacity May reduce NO <sub>x</sub> storage capacity The zeolite structure collapses, the active species aggregate and deactivate.	[45,47,87] [57] [57,66,67]
CO	Co-adsorption with NO <sub>x</sub> Reduction of Pd cation sites at high temperature Induce the migration of Pd species	Increase NO <sub>x</sub> adsorption capacity and desorption temperature Form low-valence Pd sites and increase adsorption capacity Causes the accumulation of Pd species	[72,87] [68,90] [49,64,70]
HC	Blocked pores	Reduce adsorption capacity	[28]
CO <sub>2</sub>	N/A	Almost no impact on storage capacity	[75]

**Fig. 8.** FTIR spectra collected during step-wise addition of CO adsorption on a NO saturated 1 wt% Pd/SSZ-13 sample. Reprinted with permission [87]. Copyright 2018, American Chemical Society.

However, Khivantsev *et al.* [87] proposed a different understanding of the adsorption chemistry containing CO. The FTIR spectrum suggests that the introduction of CO resulted in the conversion of the adsorbed species formed by NO<sub>x</sub> on the Pd<sup>2+</sup> cation site (As shown in Fig. 8), which may attribute to the co-adsorption complex of CO and NO, expressed as Pd(II)(NO)(CO). The higher stability of this mixed carbonyl–nitrosyl Pd complex provides a new explanation for the increase of NO<sub>x</sub> capacity. In the following research, a similar mixed carbonyl–nitrosyl Pd complex was also observed on the Pd/BEA [72]. This suggests that this CO–NO co-adsorption mechanism may be widely present in Pd/zeolite materials.

All in all, there are two mechanisms to explain the effect of CO on the performance of Pd/zeolite PNA. The co-adsorption mechanism is strongly supported by FTIR. Also, the mechanism of Pd<sup>2+</sup> reduction has certain rationality and evidence support. In addition, some previous reports also support the reduction of Pd<sup>2+</sup> sites in the presence of CO [45,47,49,64]. However, these two mechanisms do not contradict each other, they may act on the Pd species at the ion-exchange site at the same time and dominate the Pd/zeolite PNA performance under different working conditions.

#### 4.3.3. Effect of other components on the PNA performance of Pd/zeolite

In addition to H<sub>2</sub>O and CO, other exhaust components may also affect the adsorption behavior of PNA. The influence of O<sub>2</sub> on the adsorption behavior of NO<sub>x</sub> is worthy of being investigated because of the lean burn operating characteristics of diesel engines. Khivantsev *et al.* studied the effect of O<sub>2</sub> on the adsorption behav-

**Table 3**  
Possible reaction mechanism between active Pd species and exhaust gas components.

Reaction	Ref.
Z <sup>-</sup> Pd <sup>2+</sup> Z <sup>-</sup> + NO ↔ Z <sup>-</sup> Pd <sup>2+</sup> Z <sup>-</sup> – NO	[45,87]
Z <sup>-</sup> Pd <sup>2+</sup> Z <sup>-</sup> + H <sub>2</sub> O ↔ Z <sup>-</sup> Pd <sup>2+</sup> Z <sup>-</sup> – H <sub>2</sub> O	[90]
Z <sup>-</sup> Pd <sup>2+</sup> Z <sup>-</sup> + H <sub>2</sub> O + CO + NO ↔ 2Z <sup>-</sup> Pd <sup>2+</sup> (CO)(NO) + H <sub>2</sub> O	[87,90]
Z <sup>-</sup> Pd <sup>2+</sup> Z <sup>-</sup> + NO <sub>2</sub> + H <sub>2</sub> O ↔ Z <sup>-</sup> Pd <sup>2+</sup> Z <sup>-</sup> – (H <sub>2</sub> O)(NO <sub>2</sub> )	[90]
Z <sup>-</sup> Pd <sup>2+</sup> Z <sup>-</sup> + NO + CO ↔ 2Z <sup>-</sup> Pd <sup>2+</sup> (CO)(NO)	[87]
Z <sup>-</sup> Pd <sup>2+</sup> Z <sup>-</sup> + NO <sub>2</sub> ↔ Z <sup>-</sup> Pd <sup>2+</sup> Z <sup>-</sup> – NO <sub>2</sub>	[87,90]
2Z <sup>-</sup> [Pd(OH)] <sup>+</sup> + NO ↔ 2Z <sup>-</sup> Pd <sup>+</sup> + NO <sub>2</sub> + H <sub>2</sub> O	[45]
Z <sup>-</sup> [Pd(OH)] <sup>+</sup> + NO ↔ Z <sup>-</sup> [Pd(OH)] <sup>+</sup> – NO	[87,90]
Z <sup>-</sup> [Pd(OH)] <sup>+</sup> + H <sub>2</sub> O ↔ Z <sup>-</sup> [Pd(OH)] <sup>+</sup> – H <sub>2</sub> O	[90]
Z <sup>-</sup> [Pd(OH)] <sup>+</sup> + NO <sub>2</sub> + H <sub>2</sub> O ↔ Z <sup>-</sup> Pd <sup>2+</sup> Z <sup>-</sup> – (H <sub>2</sub> O)(NO <sub>2</sub> )	[90]
Z <sup>-</sup> Pd <sup>+</sup> + NO ↔ Z <sup>-</sup> Pd <sup>+</sup> – NO	[47]
Z <sup>-</sup> Pd <sup>+</sup> + H <sub>2</sub> O ↔ Z <sup>-</sup> Pd <sup>+</sup> – (H <sub>2</sub> O)	[47]
2Z <sup>-</sup> Pd <sup>+</sup> + Z <sup>-</sup> H <sup>+</sup> – H <sub>2</sub> O + 0.5O <sub>2</sub> ↔ 2Z <sup>-</sup> [Pd(OH)] <sup>+</sup> + Z <sup>-</sup> H <sup>+</sup>	[90]
2PdO + O <sub>2</sub> ↔ 2PdO <sub>2</sub>	[47]
PdO + H <sub>2</sub> O ↔ Pd(OH) <sub>2</sub>	[47]
PdO <sub>2</sub> + NO ↔ PdO + NO <sub>2</sub>	[47]
PdO <sub>2</sub> + H <sub>2</sub> O ↔ PdO <sub>2</sub> – H <sub>2</sub> O	[47]

ior of Pd/SSZ-13, a new adsorption route was proposed under the presence of O<sub>2</sub>. They pointed out that O<sub>2</sub> can promote NO<sup>+</sup> formation, and result in the increase of NO<sub>x</sub> storage capacity. In addition, the HCs produced by incomplete combustion of fuel are also investigated, the reduction of NO<sub>x</sub> storage capacity caused by coking was confirmed [28]. In another hand, the influence of CO<sub>2</sub> was also investigated by a similar method [75], however, there is insufficient evidence to show the influence of CO<sub>2</sub> introduction on the NO<sub>x</sub> storage behavior of Pd/zeolite system.

In summary, the adsorption chemistry of Pd/zeolite PNA is complex. This is due to the complex exhaust gas composition and the migration and transformation of active sites. Nevertheless, some researchers have systematically studied the adsorption chemistry of Pd/zeolite under the exhaust condition and some mechanistic schemes have been proposed [47,90]. Here, we summarize the possible adsorption reaction between active Pd species and exhaust gas components, as shown in Table 3.

#### 4.4. The effect of various factors in the work environment on long-term work

The working condition of PNA materials is harsh, because it is installed upstream of the exhaust gas treatment system. Therefore, the deactivation accompanied by long-term working must be considered, we summarized the deactivation mechanism of several Pd/zeolite PNA materials, as shown in Table 4. In addition to chemical poisoning and hydrothermal aging, the reduction effect of CO in the atmosphere also needs to be considered. In this part, the deactivation mechanisms and some possible countermeasures of Pd/zeolite PNA are given.

**Table 4**

The threat PNA faces in the exhaust gas working environment.

Deactivation threaten	Threatening species	Deactivation mechanism	Ref.
Chemistry Poisoning	SO <sub>2</sub>	Form sulfate species and block pores	[28]
	HCs	Block pores and reduce the specific surface area	[28]
Hydrothermal aging	H <sub>2</sub> O	Cause dealumination of framework and Pd sintering	[57,104,105]
Reducing atmosphere	CO	Inducing reduction and sintering of Pd species	[49,64,70]

#### 4.4.1. Effect of chemical poisoning on the PNA performance of Pd/zeolite

There are many components in diesel engine exhaust gas that may cause the inactivation of Pd/zeolite PNA materials, such as S, P and HCs [14,31,91–97]. To investigate the poisoning tolerance of zeolite-based PNA, Chen *et al.* [28] studied the performance degradation of Pd/zeolite and Pd/CeO<sub>2</sub> in the presence of SO<sub>2</sub> and n-C<sub>10</sub>H<sub>22</sub>. The temperature program experiment indicated that Pd/zeolite materials are much less affected than Pd/CeO<sub>2</sub>. It is worth noting that the Pd/SSZ-13 with the CHA framework showed the best poisoning tolerance among all samples, which can be attributed to the small pore size.

Currently, there are few studies on the improvement of poisoning tolerance of zeolite-based PNA materials, which may due to the short research time and the incomplete understanding of the adsorption chemistry. However, the poisoning tolerance determines the practical potential of the materials. The SO<sub>2</sub> tolerance of PNA needs particular attention, because sufficient research has proved the harm of sulfur to zeolite-based catalysts [98,99]. It was reported that the Brønsted acid sites on the zeolite framework effectively help to improve the sulfur tolerance of precious metal species, which may be attributed to the electron deficiency effect of precious metals caused by proton [100–102]. This provided some ideas for the improvement of sulfur resistance of Pd/zeolite series PNA catalysts, some strategies to increase the abundance of zeolite Brønsted acid sites may be adopted, such as reduce the SAR [81,82]. Of course, these schemes need further verification.

#### 4.4.2. Effect of hydrothermal aging on the PNA performance of Pd/zeolite

It is reported that hydrothermal aging (HTA) treatment may cause zeolite framework dealumination and collapse, which in turn lead to the loss of catalyst active species [10]. However, Kim's group found that HTA treatment can be used to activate Pd active sites and promote zeolite effectively [50,61,103]. Firstly, Pd/SSZ-13 materials synthesized by various methods were modified by HTA treatment [50]. The temperature programmed experiment indicates that the NO<sub>x</sub> storage performance of the samples has been significantly improved. The Pd species redispersion is considered to be the main reason for the activation of the catalyst, which is supported by H<sub>2</sub>-temperature programmed reduction (H<sub>2</sub>-TPR), XAFS, X-ray photoelectron spectroscopy (XPS) and DRIFTS. Energy dispersive spectrometer (EDS) and STEM also provided relatively intuitive evidence (Fig. 6.2). In addition, a schematic was given to describe the change in Pd species before and after HTA treatment, as shown in Fig. 9. However, for different zeolite supports, the opposite phenomenon of Pd species migration was observed [61]. XRD, XANES and EXAFS indicate the Pd species redispersion on ZSM-5 after anhydrous treatment and Pd species aggregation in the presence of H<sub>2</sub>O. However, the Pd/SSZ-13 samples showed a completely opposite trend. The author suggested that this interesting phenomenon attribute to the difference in Pd species mobility rate on different zeolite frameworks. This may be related to the zeolite pore size. After that, they further optimized the HTA condition (including temperature, time, H<sub>2</sub>O content, *etc.*) [103]. XRD and EXAFS were used to investigate the Pd species redispersion of

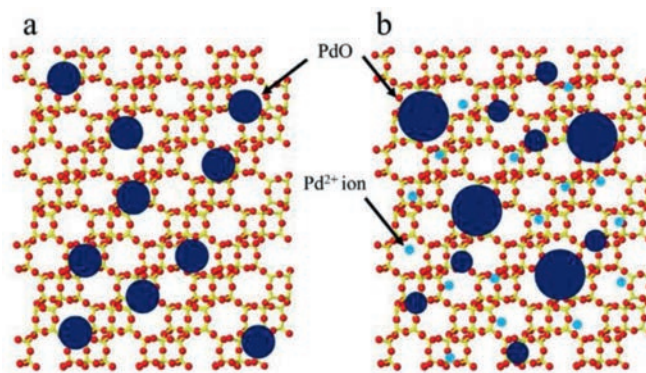


**Fig. 9.** The schematic model of the changing in Pd species in Pd/SSZ-13 before and after HTA treatment. Reprinted with permission [50]. Copyright 2017, Elsevier.

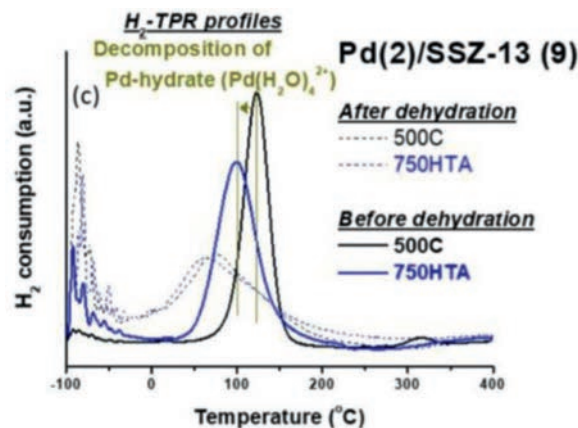


**Fig. 10.** H<sub>2</sub>-TPR profiles of Pd/SSZ-13 samples with and without the dehydration pretreatment before analysis. Reprinted with permission [62]. Copyright 2020, Elsevier.

samples obtained by post-treatment at different temperatures and durations. 15 hours of hydrothermal treatment at 750 °C was considered as the most suitable activation condition. <sup>27</sup>Al-NMR and XRD also suggest that a longer time or higher temperature may induce the dealumination of the framework and the sintering of Pd species.

In addition to inducing the redispersion of Pd species, the HTA treatment has also been reported to improve PNA performance by affecting the zeolite supports. Lee *et al.* [62] studied the improvement of Pd/SSZ-13 hydrophobicity after 750 °C with 10% H<sub>2</sub>O, which made the hydrated Pd<sup>2+</sup> cations more easily dehydrated (proved by H<sub>2</sub>-TPR, as shown in Fig. 10). This characteristic led to an increase in the adsorption capacity of Pd/SSZ-13 under the conditions that contain water.

Although HTA is proven to activate Pd/zeolite, the long-term high temperature water vapor exposure is a serious threat to the catalysts. The deactivation caused by HTA still needs to be considered. In fact, hydrothermal stability is an extremely important

parameter for exhaust gas deNO<sub>x</sub> catalysts due to the harsh working condition. Khivantsev *et al.* [67] pointed out that the prerequisite for HTA treatment redispersed Pd species is that a large amount of aggregated Pd species on the zeolite framework. If the Pd species is initially dispersed at the atomic level, the damage caused by the long-term high temperature water vapor exposure to the Pd/zeolite PNA must be considered. According to their study, sintering of Pd species on different zeolite supports caused by hydrothermal aging (750 °C, 16 h) can be observed by high-energy XRD and STEM. <sup>27</sup>Al-NMR and FTIR indicated that the dealumination and collapse of the zeolite framework are the major factors of active adsorption sites deactivation. In addition, HTA treatment has also been found to affect Pd species directly. Lee *et al.* [57] studied the deactivation of Pd/zeolite at 500 °C under the atmosphere containing NO and H<sub>2</sub>O. Interestingly, significant PdO species production was observed in Pd/ZSM-5 accompanied by catalyst deactivation, but not in Pd/SSZ-13 samples. This may be attributed to the narrow pore structure of SSZ-13 which restricts the migration of Pd species.

Although the hydrothermal deactivation mechanism of zeolite-based PNA materials was investigated, but few effective strategies to improve hydrothermal stability have been proposed. The HTA deactivation mechanism of Pd promoted zeolite may be analogous to zeolite-based SCR catalyst [104,105]. Therefore, some strategies for improving the hydrothermal stability of Cu promoted zeolite may be used for reference, for example, selected to have a smaller pore size of the zeolite as a carrier [18,58,60]. In addition, it has been reported that the pore structure may also affect the hydrothermal stability. Shan *et al.* [66] compared the hydrothermal stability of Pd modified zeolite with different topologies (AEI, CHA and RTH, with similar pore size). Pd/AEI with three-dimensional and tortuous pore showed the best NO<sub>x</sub> storage performance after 800 °C HTA treatment. Besides, Wang *et al.* [106] proposed that Cu<sup>2+</sup> cations at the ion-exchange site contribute to the stability of the SAPO-34 framework. Therefore, it remains to be verified that metal cations affect the hydrothermal stability of zeolite-based PNA.

#### 4.4.3. Pd/zeolite PNA deactivation caused by CO reduction

The effect of CO on NO<sub>x</sub> adsorption is discussed in part 4.3.2. However, the long-term CO exposure is considered as a threat to Pd/zeolite PNA due to its reducibility. Ryou *et al.* [49] studied the effect of reducing atmosphere to Pd/SSZ-13. XRD pattern indicates that the SSZ-13 framework maintains stability under 900 °C. However, aggregation of Pd species was observed in the presence of CO despite only 500 °C. Comparatively, no significant Pd aggregation was observed even at 700 °C under the H<sub>2</sub> atmosphere (proven by STEM, as shown in Fig. 6.3). The authors attributed this interesting phenomenon to differences in the effect of CO on the migration rate of Pd species. The mobility of Pd increases arising from the formation of Pd-carbonyl resulted in severe sintering of Pd species outside the framework. CO-induced Pd species sintering on mesoporous zeolite-based PNA was also reported by Bello *et al.* [64]. The aggregation of Pd species induced by CO aging is confirmed in Pd/ZSM-5 and Pd/MCM-22. Subsequently, HTA treatment is used to reactivate Pd adsorption sites, Pd/ZSM-5 proved to recover almost all PNA performance after HTA treatment.

All in all, the effect of CO in the exhaust gas on a PNA catalyst is bidirectional. The reduction of exhaust gas temperature and the improvement of combustion efficiency may help reduce the PNA deactivation caused by CO. Gu *et al.* [70] suggested that an efficient diesel oxidation catalyst (DOC) may effectively help the reduction of CO concentration. Besides, the regeneration of active adsorption sites at high temperatures may become another effective strategy to solve this problem.

## 5. Coupling strategies of PNA materials and SCR catalysts

PNA is a special diesel vehicle exhaust deNO<sub>x</sub> technology, which cannot remove NO<sub>x</sub> independently. It must be combined with other devices to completely eliminate adsorbed NO<sub>x</sub>. Therefore, the coupling of the PNA to other devices, such as a SCR, is another key issue. As mentioned before, PNA adsorbs NO<sub>x</sub> in the exhaust and desorbs it once the temperature meets the operating of SCR catalysts. Therefore, the simplest PNA-SCR coupling strategy is to additionally install the PNA before the SCR system. This strategy avoids changes to the existing SCR system. However, this strategy has to reserve additional space for PNA in the exhaust gas treatment system, which may bring additional design costs [107].

In order to effectively integrate SCR and PNA systems, some researchers have proposed strategies that coupling PNA materials and SCR catalysts in the same device. Selleri *et al.* [108] constructed a composite catalyst system by physically mixed the different SCR catalysts (including Fe/ZSM-5, Cu/CHA and V<sub>2</sub>O<sub>5</sub>-WO<sub>3</sub>-TiO<sub>2</sub>) and oxide-based PNA materials (including BaO/Al<sub>2</sub>O<sub>3</sub> and CeO<sub>2</sub>/Al<sub>2</sub>O<sub>3</sub>). Experiments showed that this composite system can reduce NO<sub>x</sub> emissions during “cold start” (from room temperature to 180 °C) by about 30%. This catalyst avoids the use of precious metals, thus effectively reducing the cost. However, the NO<sub>x</sub> removal efficiency and the tolerance to CO<sub>2</sub> and H<sub>2</sub>O of this catalyst need further improvement.

Similarly, researchers also proposed to couple zeolite-based PNA materials with SCR catalysts. Phillips *et al.* [109] proposed different composite strategies of Pd/zeolite and Cu/zeolite: i) The modified Cu and Pd active species on the same zeolite support; ii) coating PNA and SCR materials on the same monolithic catalyst. In more detail, the author introduces different catalyst coating schemes. Pd/zeolite and Cu/zeolite can be layered in different orders, or distributed in different areas of the same monolithic catalyst. These schemes not only provide a reference for the design of the PNA-SCR system, but also give some references for the subsequent research of PNA materials, such as improving its compatibility with the SCR catalyst. And the change in the adsorption chemistry caused by the combination of the two catalysts is another problem that needs to be considered. Recently, this strategy, so called dual-layer monolith was investigated in detail [107]. The dual-layer catalyst contains Pd/SSZ-13 and Cu/SSZ-13 with the same weight were coated monolithic catalysts. The PNA materials were coated on the bottom layer and SCR catalyst was coated on the top layer. The SEM and EDS images suggest the layered distribution of PNA materials and SCR catalysts on cordierite monoliths, as shown in Fig. 6.4. The simulated exhaust gas test shows that the dual-layer catalyst can maintain most of the NO<sub>x</sub> storage capacity and appropriately increase the NO<sub>x</sub> desorption temperature. However, NO<sub>x</sub> storage capacity reduction after SCR testing and high-concentration CO exposure needs to be concerned. In addition, the distribution and ratio of the two catalysts can also be further optimized.

In summary, the concept of an integrated PNA-SCR catalyst was proposed. It should be noted that the PNA-SCR composite is different from NSR technology, because the lean-rich cycle is not necessary. However, a separate design may also have some advantages, such as convenient maintenance and replacement of devices. On the other hand, if a bypass can be designed to prohibit exhaust gas from passing through the PNA device after the “cold start” phase, it can effectively reduce the exposure time of the PNA material and extend its life.

## 6. Conclusions and prospects

Zeolite-based PNA has received widespread attention once it was proposed, the Pd/zeolites are still considered to be the most

potential candidate for PNA materials. At present, highly dispersed Pd/zeolite with smaller pores has been developed, and its potential is widely recognized due to its excellent hydrothermal stability and anti-poisoning performance. In this review, we summarized the adsorption chemistry, structure-activity relationship and threats in the long-term use of Pd/zeolite PNA materials.

Based on the existing research results, we put forward a prospect for the future development of zeolite-based PNA catalysts: i) Adsorption chemistry: Although the interaction between the active site and NO<sub>x</sub>, CO and H<sub>2</sub>O has been initially proved, a more detailed mechanism still need to be verified, especially the interaction between active sites and exhaust components in complex conditions. Kinetic methods and DFT calculations may become important research tools. ii) Material improvement: zeolite-based PNA with small pores have obvious advantages. Simultaneously, non-precious metal active species may receive more attention due to their low cost. In short, understanding the structure-activity relationship will be the focus of material optimization. iii) Synthesis methods: Despite the methods for preparing high dispersion Pd/zeolite PNA with high Pd dispersion have been proposed, these methods are too cumbersome or produce more pollution. Some simple and efficient methods (such as one-pot method) will be adopted. iv) Long-term performance: The deactivation mechanism will be further investigated, and some strategies which used in other metal modified zeolite catalysts may be a reference.

### Declaration of competing interest

The authors declare that they have no known competing financial interests or personal relationships that could have appeared to influence the work reported in this paper.

### Acknowledgments

The authors gratefully acknowledge financial support from the National Natural Science Foundation of China (No. 52000084), the China Postdoctoral Science Foundation (No. 2019M662630) and National Engineering Laboratory for Mobile Source Emission Control Technology (No. NELMS2018A08).

### References

- [1] S. Mohan, P. Dinesha, S. Kumar, *Chem. Eng. J.* 384 (2020) 123253.
- [2] V. Praveena, M.L.J. Martin, *J. Energy Inst.* 91 (2018) 704–720.
- [3] F.Y. Gao, X.L. Tang, H.H. Yi, et al., *Catalysts* 7 (2017) 199.
- [4] C.V. Raghunath, M.K. Mondal, *Chem. Eng. J.* 314 (2017) 537–547.
- [5] F. Gholami, M. Tomas, Z. Gholami, M. Vakili, *Sci. Total Environ.* 714 (2020) 136712.
- [6] A. Faustini, R. Rapp, F. Forastiere, *Eur. Respir. J.* 44 (2014) 744–753.
- [7] P. Gilot, M. Guyon, B.R. Stanmore, *Fuel* 76 (1997) 507–515.
- [8] B. Giechaskiel, R. Suarez-Bertoa, T. Lahde, et al., *Environ. Res.* 166 (2018) 298–309.
- [9] L.Q. He, S.J. Zhang, J.N. Hu, et al., *Environ. Pollut.* 262 (2020) 114280.
- [10] S. Brandenberger, O. Krocher, A. Tissler, R. Althoff, *Catal. Rev.* 50 (2008) 492–531.
- [11] T.V. Johnson, *Int. J. Engine. Res.* 10 (2009) 275–285.
- [12] A. Walker, *Top. Catal.* 59 (2016) 695–707.
- [13] J.H. Li, H.Z. Chang, L. Ma, J.M. Hao, R.T. Yang, *Catal. Today* 175 (2011) 147–156.
- [14] Z. Chen, C. Fan, L. Pang, et al., *Appl. Catal. B* 237 (2018) 116–127.
- [15] Z. Chen, Q. Liu, L. Guo, et al., *Appl. Catal. B* 286 (2021) 199816.
- [16] F.D. Liu, W.P. Shan, X.Y. Shi, C.B. Zhang, H. He, *Chin. J. Catal.* 32 (2011) 1113–1128.
- [17] L.P. Han, S.X. Cai, M. Gao, et al., *Chem. Rev.* 119 (2019) 10916–10976.
- [18] J.H. Kwak, R.G. Tonkyn, D.H. Kim, J. Szanyi, C.H.F. Peden, *J. Catal.* 275 (2010) 187–190.
- [19] D.W. Fickel, E. D'Addio, J.A. Lauterbach, R.F. Lobo, *Appl. Catal. B* 102 (2011) 441–448.
- [20] L.M. Ren, L.F. Zhu, C.G. Yang, et al., *Chem. Commun.* 47 (2011) 9789–9791.
- [21] R. Sala, J. Krasowski, J. Dzida, *MATEC Web Conf.* 118 (2017) 00035.
- [22] M. Moliner, A. Corma, *React. Chem. Eng.* 4 (2019) 223–234.
- [23] M. Weilenmann, J.Y. Favez, R. Alvarez, *Atmos. Environ.* 43 (2009) 2419–2429.
- [24] A. Roberts, R. Brooks, P. Shipway, *Energy Convers. Manage.* 82 (2014) 327–350.
- [25] H.Y. Chen, U.S. Patent Application, 2012, 2012/0308439.
- [26] F.M. McKenna, U.S. Patent (2015) 9005560 B2.
- [27] R. Rajaram, F.M. McKenna, H.Y. Chen, D. Liu, U.S. Patent Application 2015, 2015/0157982 A1.
- [28] H.Y. Chen, J.E. Collier, D.X. Liu, et al., *Catal. Lett.* 146 (2016) 1706–1711.
- [29] Q.R. Jiang, C. Wang, M.Q. Shen, et al., *Catal. Commun.* 125 (2019) 103–107.
- [30] Y. Gu, W.S. Epling, *Appl. Catal. A* 570 (2019) 1–14.
- [31] J. Lee, J.R. Theis, E.A. Kyriakidou, *Appl. Catal. B* 243 (2019) 397–414.
- [32] M. Iwamoto, H. Furukawa, Y. Mine, et al., *J. Chem. Soc. Chem. Commun.* (1986) 1272–1273.
- [33] W.S. Epling, L.E. Campbell, A. Yezerets, N.W. Currier, J.E. Parks, *Catal. Rev.* 46 (2004) 163–245.
- [34] S. Roy, A. Baiker, *Chem. Rev.* 109 (2009) 4054–4091.
- [35] K. Eranen, L.E. Lindfors, F. Klingstedt, D.Y. Murzin, *J. Catal.* 219 (2003) 25–40.
- [36] K. Shimizu, A. Satsuma, *Phys. Chem. Chem. Phys.* 8 (2006) 2677–2695.
- [37] J. Shibata, M. Hashimoto, K. Shimizu, et al., *J. Phys. Chem. B* 108 (2004) 18327–18335.
- [38] P.G. Savva, C.N. Costa, *Catal. Rev.* 53 (2011) 91–151.
- [39] Y. Xin, Q. Li, Z.L. Zhang, *ChemCatChem* 10 (2018) 29–41.
- [40] K. Zhang, L.Y. Fan, D.W. Qu, *Appl. Mech. Mater.* 511–512 (2014) 811–814.
- [41] S. Jones, Y.Y. Ji, M. Crocker, *Catal. Lett.* 146 (2016) 909–917.
- [42] Y.Y. Ji, D.Y. Xu, S.L. Bai, et al., *Ind. Eng. Chem. Res.* 56 (2017) 111–125.
- [43] S. Jones, Y. Ji, A. Bueno-Lopez, Y. Song, M. Crocker, *Emiss. Control Sci. Technol.* 3 (2016) 59–72.
- [44] J.R. Theis, C.K. Lambert, *Catal. Today* 258 (2015) 367–377.
- [45] Y. Zheng, L. Kovarik, M.H. Engelhard, et al., *J. Phys. Chem. C* 121 (2017) 15793–15803.
- [46] B.J. Adelman, W.M.H. Sachtler, *Appl. Catal. B* 14 (1997) 1–11.
- [47] M. Ambast, K. Karinshak, B.M.M. Rahman, L.C. Grabow, M.P. Harold, *Appl. Catal. B* 269 (2020).
- [48] K. Okumura, J. Amano, N. Yasunobu, M. Niwa, *J. Phys. Chem. B* 104 (2000) 1050–1057.
- [49] Y. Ryou, J. Lee, Y. Kim, et al., *Appl. Catal. A* 569 (2019) 28–34.
- [50] Y. Ryou, J. Lee, S.J. Cho, et al., *Appl. Catal. B* 212 (2017) 140–149.
- [51] K.I. Hadjiivanov, *Catal. Rev.* 42 (2000) 71–144.
- [52] K. Chakarova, E. Ivanova, K. Hadjiivanov, D. Klissurski, H. Knozinger, *Phys. Chem. Chem. Phys.* 6 (2004) 3702–3709.
- [53] F. Lonyi, H.E. Solt, J. Valyon, et al., *Appl. Catal. B* 100 (2010) 133–142.
- [54] A. Porta, T. Pellegrinelli, L. Castoldi, et al., *Top. Catal.* 61 (2018) 2021–2034.
- [55] D.H. Mei, F. Gao, J. Szanyi, Y. Wang, *Appl. Catal. A* 569 (2019) 181–189.
- [56] Q.J. Yu, X.Y. Chen, A. Bhat, et al., *Chem. Eng. J.* 399 (2020) 125727.
- [57] J. Lee, Y. Kim, S. Hwang, et al., *Catal. Today* 360 (2021) 350–355.
- [58] A.M. Beale, F. Gao, I. Lezcano-Gonzalez, et al., *Chem. Soc. Rev.* 44 (2015) 7371–7405.
- [59] L.J. Xie, F.D. Liu, L.M. Ren, et al., *Environ. Sci. Technol.* 48 (2014) 566–572.
- [60] J.H. Wang, H.W. Zhao, G. Haller, Y.D. Li, *Appl. Catal. B* 202 (2017) 346–354.
- [61] J. Lee, Y. Ryou, S. Hwang, et al., *Catal. Sci. Technol.* 9 (2019) 163–173.
- [62] J. Lee, J. Kim, Y. Kim, et al., *Appl. Catal. B* 277 (2020) 119190.
- [63] J. Lee, Y. Ryou, S.J. Cho, et al., *Appl. Catal. B* 226 (2018) 71–82.
- [64] E. Bello, V.J. Margarit, E.M. Gallego, et al., *Micropor. Mesopor. Mat.* 302 (2020) 110222.
- [65] J.A.P. Rabo, M.L. Poutsma, G.W. Skeels, *Catal. Proc. Int. Congr.* 5th 2 (1973) 1353–1363.
- [66] Y.L. Shan, Y. Sun, Y.B. Li, et al., *Top. Catal.* 63 (2020) 944–953.
- [67] K. Khivantsev, N.R. Jaegers, L. Kovarik, et al., *Emiss. Control Sci. Technol.* 6 (2019) 126–138.
- [68] A. Vu, J.Y. Luo, J.H. Li, W.S. Epling, *Catal. Lett.* 147 (2017) 745–750.
- [69] S.A. Malamis, M.P. Harold, W.S. Epling, *Ind. Eng. Chem. Res.* 58 (2019) 22912–22923.
- [70] Y. Gu, R.P. Zelinsky, Y.R. Chen, W.S. Epling, *Appl. Catal. B* 258 (2019) 118032.
- [71] B. Zhang, M. Shen, J. Wang, et al., *Catalysts* 9 (2019) 247.
- [72] K. Khivantsev, N.R. Jaegers, L. Kovarik, et al., *Appl. Catal. A* 569 (2019) 141–148.
- [73] M. Jiang, J. Wang, J. Wang, M. Shen, *Materials (Basel)* 12 (2019) 1045.
- [74] R.F. Ilmasani, J. Woo, D. Creaser, L. Olsson, *Ind. Eng. Chem. Res.* 59 (2020) 9830–9840.
- [75] O. Mihai, L. Trandafilovic, T. Wentworth, F.F. Torres, L. Olsson, *Top. Catal.* 61 (2018) 2007–2020.
- [76] K. Khivantsev, N.R. Jaegers, L. Kovarik, et al., *Angew. Chem. Int. Ed.* 57 (2018) 16672–16677.
- [77] R.L. Wadlinger, L. Rosinski, G.T. Kerr, E.J. Rosinski, 1964.
- [78] M. Nakai, K. Miyake, R. Inoue, et al., *Micropor. Mesopor. Mat.* 273 (2019) 189–195.
- [79] J. Zhu, Z.D. Liu, S. Sukenaga, et al., *Micropor. Mesopor. Mat.* 268 (2018) 1–8.
- [80] A. Corma, *J. Catal.* 216 (2003) 298–312.
- [81] S. Mintova, V. Valtchev, T. Onfroy, et al., *Micropor. Mesopor. Mat.* 90 (2006) 237–245.
- [82] L. Shirazi, E. Jamshidi, M.R. Ghasemi, *Cryst. Res. Technol.* 43 (2008) 1300–1306.
- [83] S.A. Bates, A.A. Verma, C. Paolucci, et al., *J. Catal.* 312 (2014) 87–97.
- [84] I. Friberg, N. Sadokhina, L. Olsson, *Appl. Catal. B* 250 (2019) 117–131.
- [85] F. Gao, N.M. Washton, Y.L. Wang, et al., *J. Catal.* 331 (2015) 25–38.
- [86] S. Han, J. Cheng, C.K. Zheng, et al., *Appl. Surf. Sci.* 419 (2017) 382–392.
- [87] K. Khivantsev, F. Gao, L. Kovarik, Y. Wang, J. Szanyi, *J. Phys. Chem. C* 122 (2018) 10820–10827.
- [88] N.M. Markovic, T.J. Schmidt, V. Stamenkovic, P.N. Ross, *Fuel Cells* 1 (2001) 105–116.

- [89] E. Antolini, *Energy Environ. Sci.* 2 (2009) 915–931.
- [90] A. Gupta, S.B. Kang, M.P. Harold, *Catal. Today* 360 (2021) 411–425.
- [91] W.P. Shan, H. Song, *Catal. Sci. Technol.* 5 (2015) 4280–4288.
- [92] C. Gao, J.W. Shi, Z.Y. Fan, G. Gao, C.M. Niu, *Catalysts* 8 (2018) 11.
- [93] H.E. van der Bij, B.M. Weckhuysen, *Chem. Soc. Rev.* 44 (2015) 7406–7428.
- [94] L. Ma, W.K. Su, Z.G. Li, et al., *Catal. Today* 245 (2015) 16–21.
- [95] A. Wang, L. Olsson, *Chem. Eng. J.* 395 (2020) 125048.
- [96] A. Wang, K. Xie, D. Bernin, et al., *Appl. Catal. B* 269 (2020) 118781.
- [97] L. Yan, Y. Ji, P. Wang, et al., *Environ. Sci. Technol.* 54 (2020) 9132–9141.
- [98] L. Zhang, D. Wang, Y. Liu, et al., *Appl. Catal. B* 156–157 (2014) 371–377.
- [99] K. Wijayanti, K. Leistner, S. Chand, et al., *Catal. Sci. Technol.* 6 (2016) 2565–2579.
- [100] A. Corma, A. Martinez, V. MartinezSoria, *J. Catal.* 169 (1997) 480–489.
- [101] H. Yasuda, T. Sato, Y. Yoshimura, *Catal. Today* 50 (1999) 63–71.
- [102] Y. Yoshimura, H. Yasuda, T. Sato, N. Kijima, T. Kameoka, *Appl. Catal. A* 207 (2001) 303–307.
- [103] Y. Ryou, J. Lee, H. Lee, C.H. Kim, D.H. Kim, *Catal. Today* 320 (2019) 175–180.
- [104] K. Rahkamaa-Tolonen, T. Maunula, M. Lomma, M. Huuhtanen, R.L. Keiski, *Catal. Today* 100 (2005) 217–222.
- [105] J.H. Kwak, D. Tran, S.D. Burton, et al., *J. Catal.* 287 (2012) 203–209.
- [106] J. Wang, D.Q. Fan, T. Yu, et al., *J. Catal.* 322 (2015) 84–90.
- [107] A. Wang, K. Xie, A. Kumar, K. Kamasamudram, L. Olsson, *Catal. Today* 360 (2021) 356–366.
- [108] T. Selleri, F. Gramigni, I. Nova, et al., *Catal. Sci. Technol.* 8 (2018) 2467–2476.
- [109] P.R. Phillips, G.R. Chandler, A.N.M. Green, et al., U.S. Patent Application 2016, 2016/0136626.